A Potential Approach for Converting Rubber Waste into a Low-Cost Polymeric Adsorbent for Removing Methylene Blue from Aqueous Solutions

Muhammad Aliyu[1,2], Abdul Halim Abdullah[1,3*], and Mohamed Ibrahim bin Mohamed Tahir[1]

[1]*Department of Chemistry, Faculty of Science, Universiti Putra Malaysia, 43400 UPM Serdang, Selangor, Malaysia*

[2]*Department of Chemistry, Faculty of Natural and Applied Science, Sule Lamido University, Kafin Hausa, Jigawa State, Nigeria*

[3]*Institute of advanced Technology, Universiti Putra Malaysia, 43400 Serdang, Selangor Darul Ehsan Malaysia*

Corresponding author:

email: halim@upm.edu.my

Received: October 9, 2021
Accepted: February 18, 2022

DOI: 10.22146/ijc.69674

Abstract: *Exploiting waste materials to make cost-effective adsorbents and waste management methods are gaining more attention. In the current study, rubber wastes derived from dipping tank coagulum (DTC) in the glove manufacturing industry were converted into a novel polymeric-adsorbent via a simple sulfonation reaction with concentrated sulphuric acid and was used for the adsorption of methylene blue (MB) dye from aqueous solutions commonly found in contaminated waters. FT-IR, EDX, FESEM, and BET techniques were used to characterize the rubber waste before and after modification. The highest MB removal efficiency of 99.03% was achieved in the condition of initial concentration, adsorbent dosage, pH, contact time, and temperature were 15 mg/L, 30 mg, pH 7, 300 min, and 25 °C, respectively. The adsorption of MB was analyzed using experimental data fitted in a monolayer isotherms model with a maximum adsorption capacity of 119 mg/g. The kinetic model was revealed to agree with the pseudo-second-order kinetic model. Furthermore, SRW retained 90.45% of the removal percentage after four cycles of the repeated adsorption-desorption process. Conclusively, these findings suggest that rubber waste could be a suitable low-cost adsorbent to remove organic dyes from polluted water.*

Keywords: *methylene blue; adsorption; rubber waste; polymeric materials; environmental remediation*

■ INTRODUCTION

Malaysia is amongst the world's largest manufacturers and suppliers of rubber products such as examination and surgical gloves, which account for more than 70% of total rubber product exports and almost 60% of global consumption [1]. The rubber products market has expanded significantly in recent years to meet worldwide demand. The global rubber market was worth $29.8 billion in 2018 and is predicted to grow by 5.2% between 2019 and 2026 [2]. Despite having a substantial market share in global rubber products exports, the rubber glove manufacturing industry currently faces the difficulty of regulating massive volumes of waste generated throughout the rubber glove manufacturing process [3]. In addition, rubber latex manufacturing plants generate large amounts of formulated rubber latex waste, known as dipping tank coagulum (DTC), mostly created by rubber glove dipping tanks. It is classified as scheduled waste and must be disposed of via incineration as scheduled waste under the Environmental Quality Act [4]. However, incineration of these solid rubber wastes has a severe environmental impact since they pollute land and air [5]. Therefore, an important topic addressed in this research is a new method of converting rubber waste into usable and sustainable materials for the benefit of the environment.

Methylene blue (MB) is a cationic dye whose component is a crystalline dark green powder with a bronze luster [6]. Although MB is not regarded as acutely toxic, it does have negative effects. Inhaling MB dye directly may induce breathing difficulties, while

ingestion may cause nausea, vomiting, and diarrhea [7]. In addition, a substantial amount of MB inhalation may potentially result in methemoglobinemia, jaundice, quadriplegia, cyanosis, and mental disorientation [8-10]. Furthermore, MB is a high-demand material in the textile industry, which is utilized in silk and cotton painting [11]. Therefore, the removal of MB from wastewater using cost-effective adsorbents is a key environmental concern. For the removal of dyes, several techniques such as membrane filtration [12], biosorption [13], adsorption [14], and photocatalytic processes [15] are frequently used. Among the techniques mentioned, the adsorption method is considered as the most outstanding technique since it is the simplest, cheapest, and most successful technique for generating high-quality dye effluents. Agricultural bio-sorbents such as [16], weeping willow [17], and mango leaf powder [18], as well as industrial wastes such as red mud [19] and fly ash [20], have recently been used as non-conventional adsorbents.

There is yet to be any research on the use of rubber waste obtained from DTC in the rubber industry as a polymeric adsorbent for adsorption and reusability. Therefore, the focus of this research paper was on the MB dye adsorption experiments and the reusability of rubber waste as polymeric adsorbents. The rubber waste was functionalized via a sulfonation process with concentrated sulfuric acid. All available characterizations were employed to analyze the functionality, morphology, elemental composition, and textual properties of the polymeric material before and after modification. In addition, the influence of adsorbent dose, solution pH, initial MB concentration, and contact time on MB adsorption were investigated. Furthermore, to analyze the adsorption equilibrium and evaluate the adsorption mechanism, adsorption data were fitted with different isotherms (Langmuir and Freundlich isotherm models) as well as kinetic models (pseudo-first and pseudo-second-order kinetic models). Afterwards, the reusability of the adsorbent was investigated using several types of desorbing solutions (0.1 M NaOH, 0.1 M HCl, and distilled water).

■ EXPERIMENTAL SECTION

Materials

The rubber waste (RW) used in this study was obtained from the dipping tank coagulum (DTC), collected from a glove manufacturing factory in Selangor, Malaysia. The chemicals used in this study include H_2SO_4 (98% purity Merck, Germany), NaOH (99% purity Merck, Germany), $C_{16}H_{18}N_3SCl$ (95% purity Sigma Aldrich, China), and CH_3OH (99% purity Sigma Aldrich, China). All reagents were of analytical grade and applied without any further purification. Deionized and distilled water were produced from the Millipore Alpha Q system and distiller, respectively. Aqueous solutions were prepared with distilled water.

Instrumentation

Field Emission Scanning Electron Microscopy (FESEM) was used to analyze the microstructure and morphology of materials (FEI NOVA SEM 230). Energy-dispersive X-ray spectroscopy was used to determine the elemental composition of the samples (EDX). Fourier transform infrared (FTIR) spectroscopy was performed (IRTracer-100) with a Shimadzu model spectrophotometer to identify the functional groups of the polymeric materials. The spectra were examined in the 4000–400 cm^{-1} wavenumber region. Polymeric materials' surface area and pore characteristics were investigated using the Brunauer-Emmett-Teller (BET) methodology for N_2 adsorption/desorption (Micromeritics ASAP2020).

Procedure

Modification of rubber waste

The collected rubber waste (RW) was masticated into fine particles with a mortar and pestle and sieved through a 150-mesh sieve and washed three times with distilled water to dissolve the water-soluble impurities and surface adhered particles. The solid particles were then dried in an oven at 50 °C for 5 h to remove moisture and volatile undesirable substances and later cooled to room temperature. The RW was then suspended in 50 mL

of methanol to eliminate any organic residue on the solid material's surface and oven-dried at 50 °C overnight to ensure there was no moisture on the sample. Next, 15 g of the RW was modified by suspending it in 30 mL of 75% sulfuric acid for 20 min. Then, the sulfonated rubber waste (SRW) was filtered, rinsed with excess distilled water, and neutralized with 40 mL of 5 M sodium hydroxide solution. Finally, the SRW was rinsed with deionized water until the wash water reached neutral pH before being oven-dried at 75 °C for 10 h. The modification of rubber waste via sulfonation reaction is depicted in Fig. 1.

Point of zero charges (pH_{PZC})

The pH_{PZC} of polymeric materials was determined using the pH drift method [21]. For this experiment, 40 mL of 0.1 M NaCl salt solution was placed in ten separate 50 mL beakers. The pH of the solution was adjusted to pH 2–12 using 0.1 M HCl and 0.1 M NaOH solutions. 0.1 g of polymeric materials were then added into the solution and the mixtures were stirred for 24 h. A calibrated pH meter was used to measure both the initial (pH_i) and the final pH values (pH_f). The difference in pH between the initial and final values ($pH_i - pH_f$) was plotted as a function of pH_i·pH_{PZC} is the intersection of the drawn curve with the horizontal axis.

Preparation of methylene blue stock solution and construction of calibration curve

The preparation of the methylene blue (MB) stock solution and construction of the calibration curve were conducted using the dilution series method and UV-visible spectroscopy measurements described by Temel et al. at a maximum wavelength (λ_{max}) of 664 nm, respectively [7]. In summary, the stock solution was made by dissolving 100 mg of MB in 1000 mL of distilled water. The solution for the adsorption studies was made by diluting the MB with distilled water to the desired concentration**.** The chemical calibration standard is constructed to determine the accuracy and precision of the UV-visible spectroscopy measurements based on the measurement of an unknown sample. In order to make a calibration curve for the instrument, a blank and five standards diluted from the stock solution were prepared. The MB standard solutions were prepared with different concentrations of 5, 10, 15, 20, and 25 mg/L. The absorbance value was recorded at their respective λ_{max} and was plotted against the concentration which gave a linear calibration curve with correlation coefficients (R^2) ranging from 0.999 to 1.0000.

Adsorption experiment

Adsorption studies were carried out in a batch experiment to determine the best conditions for removal processes; contact time, adsorbent dose, solution pH, and initial concentration of MB. In order to determine the adsorption equilibrium time, adsorption experiments were performed on exactly 120 mL of methylene blue solution (15 mg/L) with the dose of 30 mg in a 250 mL conical flask under 25 °C for 300 min. The conical flask was shaken by a shaker (PROTECH, Malaysia) at 150 rpm. To investigate the influence of pH on adsorption, the pH of 120 mL of MB solution (15 mg/L) was adjusted with 0.1 M HCl or 0.1 M NaOH solution to obtain solutions with pH ranging from 3 to 11, and then a 30 mg adsorbent dosage was added into the solution. To determine the effect of adsorbent dose on the MB adsorption rate, various experiments were run at optimum pH (pH 7) and adsorption equilibrium of 300 min with varied doses of adsorbent (10–50 mg). An experiment to determine the influence of initial MB concentrations solutions (5–25 mg/L) was performed using 30 mg adsorbent at pH 7 and adsorption equilibrium time of 300 min.

The final solution was filtered with Whatman filter

Fig 1. The sulfonation reaction of the rubber waste

paper and the residual concentration of the MB was measured using a UV–vis Spectrophotometer (PerkinElmer Lambda 35) at λ_{max} = 664 nm. All experiments were carried out in triplicate, and the mean and standard deviation of the results were used to make further calculations.

The adsorption capacity (Q_e) was estimated using Eq. (1), and the removal percentage was computed using Eq. (2), as shown below.

$$Q_e = \frac{(C_o - C_e) \times V}{m} \quad (1)$$

$$\text{Removal } (\%) = \frac{C_o - C_e}{C_o} \times 100 \quad (2)$$

where, C_e (mg/L) is the MB concentration in an aqueous solution at equilibrium and C_o (mg/L) is the initial MB concentration in an aqueous solution. Q_e (mg/g) is the actual amount of MB adsorbed per gram SRW at equilibrium, V (L) is the volume of MB solution, and m (g) is the weight of SRW.

Regeneration and reusability experiment

Adsorption of MB on 30 mg of SRW was performed in 120 mL of 15 mg/L of MB dye solution fixed at pH 7 at a temperature of 25 °C for reusability analysis. After the adsorption process, the used adsorbent was dried overnight at a temperature of 25 °C. After that, the adsorbent was immersed in various solutions (0.1 M NaOH, 0.1 M HCl, and distilled water) and shaken for 2 h. The SRW was then dried at room temperature (25 °C) overnight. The adsorption and washing processes were conducted four times. The experiments were carried out in triplicate, And the mean and standard deviations were reported.

■ RESULTS AND DISCUSSION

Characterization of Polymeric Adsorbent

The FTIR spectrum was used to validate the existence of various functional groups in the polymeric materials with a distinct adsorption band. Fig. 2(a–c) show the IR spectrum of RW, SRW, and SRW after MB adsorption, respectively. The IR spectrum of RW (Fig. 2(a)) show a strong spectral band detected at 3314.14 cm^{-1} which was due to O–H stretching vibration.

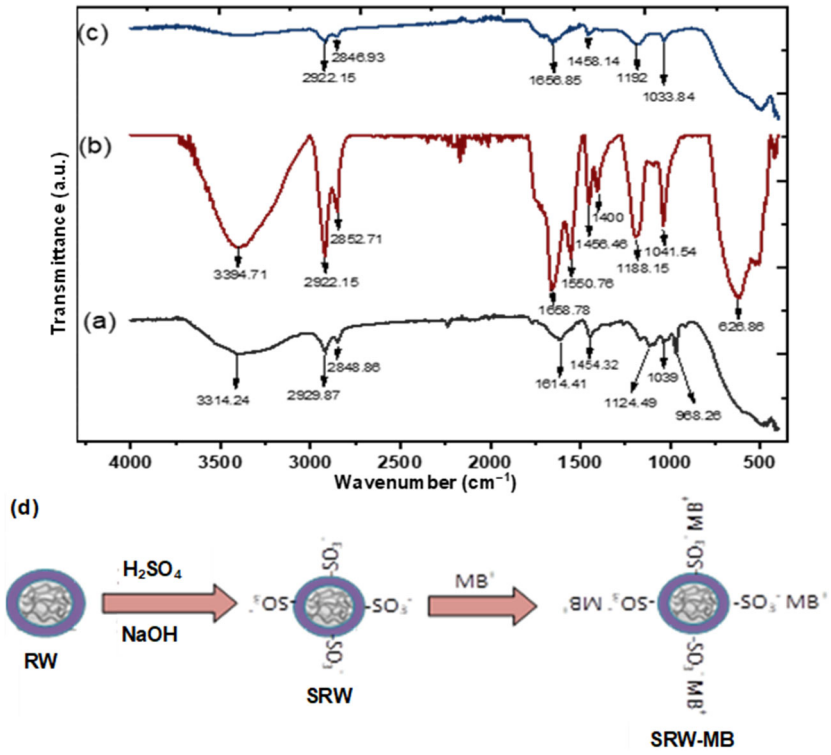

Fig 2. (a) FTIR of RW (b) SRW (c) SRW-after adsorption and (d) the mechanism of the sulfonate group during the adsorption process

Intense spectral bands observed at 2929.87 and 2848.87 cm^{-1} were attributed to C–H stretching vibration, while peaks at 1614.41 and 1454.22 cm^{-1} were assigned to the C=C stretching vibration for alkene and aromatic, respectively. The peak at 1124.49 cm^{-1} was caused by C–O stretching vibration. The intense spectra band observed at 1039.63 cm^{-1} corresponded to the stretching vibration of sulfoxide S=O, while the spectra band observed at 966.26 cm^{-1} corresponded to the bending vibration of C=C alkene (disubstituted trans). The FTIR spectrum of SRW, depicted in Fig. 2(b), showed multiple intense peaks with several new peaks and a minor transition compared to the FTIR spectrum of RW. The presence of sulfonate groups ($-SO_3^-$) in the recent spectrum peak at 1400 cm^{-1} indicates that the sulfonate group was added during the sulfonation reaction. The FTIR spectrum of SRW after MB adsorption (Fig. 2(c)) did not show the peak of 1400 cm^{-1}. The results imply that the $-SO_3^-$ functional group plays an important role in the adsorption process. Fig. 2(d) depicts the mechanism of the sulfonate group during the adsorption process.

The point of zero charge pH (pH_{PZC}) of polymeric adsorbents was used to determine the variation in the magnitude of the surface charge caused by various functional groups present on the surface of the polymeric adsorbents [21]. As revealed in Fig. 3, the pH_{PZC} values for RW and SRW were 8.78 and 2.62, respectively. The pH_{PZC} of SRW was higher than the neutral pH point, indicating that the SRW surface was negatively charged due to the presence of a sulfonate group, resulting in preferred cation adsorption [22]. On the other hand, the surface of RW was positively charged due to pH_{PZC} < pH and protonated by abundant H^+ ions.

The surface morphology and particle size distribution of polymeric materials were characterized by field emission scanning electron microscopy (FESEM). The FESEM images revealed in Fig. 4(a) and (b), show that the RW and SRW materials were comprised from particles of spherical and irregular shapes. Fig. 4(a) depicts the average size distribution of

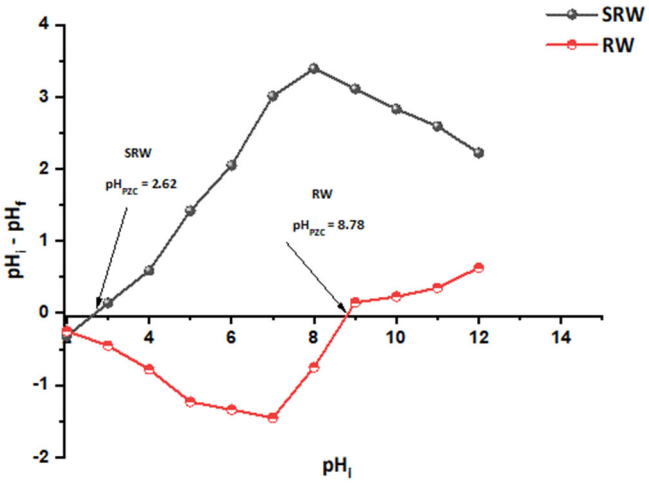

Fig 3. pH of point of zero charges of RW and SRW

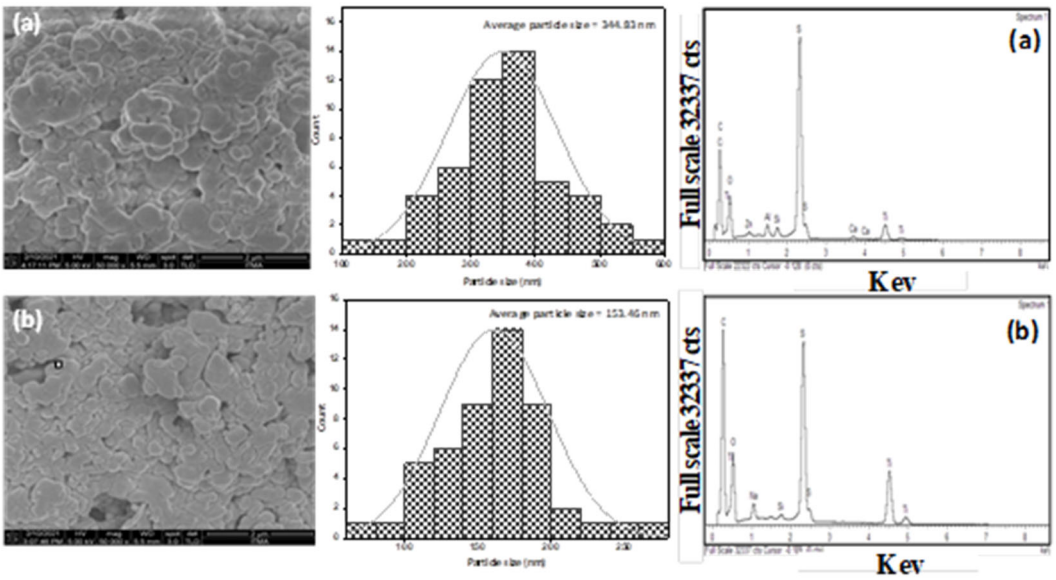

Fig 4. FESEM images and EDX of (a) RW and (b) SRW

RW (344.83 ± 82.61 nm), which was considerably larger than the particle size of SRW (153.46 ± 33.20 nm) as shown in Fig. 4(b). This might be because the RW material had been modified and undesirable elements had been removed.

The EDX spectrum of polymeric materials is depicted in Fig. 4(a) and (b). As shown in Fig. 4(a), the rubber waste (RW) contains a variety of elements, including carbon (C), oxygen (O), silicon (Si), sulfur (S), calcium (Ca), zinc (Zn), aluminum (Al), and titanium (Ti). The major constituents of RW were C, S, and O, while the remaining elements may be the product additives, as seen in Table 1. The EDX spectrum of SRW is displayed in Fig. 4(b), and the presence of C, O, S, Si, Ti and Na, as well as the percentage composition of the elements are shown in Table 1. The oxygen percentage composition increased, which might be attributed to sulfonation. Some of the elements in RW were not detected in SRW or decreased in percentage, which might be due to leaching during the acid treatment process [23]. The presence of sodium in SRW was attributed to the neutralization process after the acid treatment of RW. Furthermore, the percentage of sulfur ingredients in SRW had dropped. This could be attributed to the increased oxygen content of the RW material.

The Brunauer-Emmett-Teller (BET) surface area, total pore volume, and average pore size of RW and SRW that were determined by nitrogen adsorption-desorption are shown in Table 2. According to IUPAC, RW and SRW have a narrow pore distribution with an average pore size of 6.96 and 9.39 nm respectively and are considered as mesoporous materials. Both polymeric materials have a considerably high surface area compared to garlic peel (4.23 m^2/g) [24] and Litchi peel biomass (3.73 m^2/g) [25].

Adsorption Studies

A preliminary experiment was carried out for the adsorption of MB over unmodified rubber waste, and it was discovered that just 2.02% of the MB was removed. However, SRW demonstrated that MB was removed at more than 99.5%, due to the presence of a sulfonate group on the surface of SRW. Therefore, the following variables affecting the adsorption process were investigated:

Effect of contact time

The contact time is one of the most important elements that influence the removal percentage, adsorption capacity, and the time required to reach equilibrium [26]. A series of experiments were carried out

Table 1. Elemental compositions of RW and SRW

Element composition	Symbol	RW	SRW
		Atomic %	Atomic %
Carbon	C	70.43	69.72
Oxygen	O	17.18	20.24
Aluminum	Al	0.46	-
Silicon	Si	0.36	0.13
Sulphur	S	9.88	5.96
Calcium	Ca	0.15	-
Titanium	Ti	1.4	3.3
Zinc	Zn	1.14	-
Sodium	Na	-	0.66
Total		100	100

Table 2. The results of the BET analysis

Feature	RW	SRW
BET surface area (m^2/g)	7.87	5.94
Total pore volume (cm^3/g)	0.01371	0.01398
Average Pore size (nm)	6.96	9.39

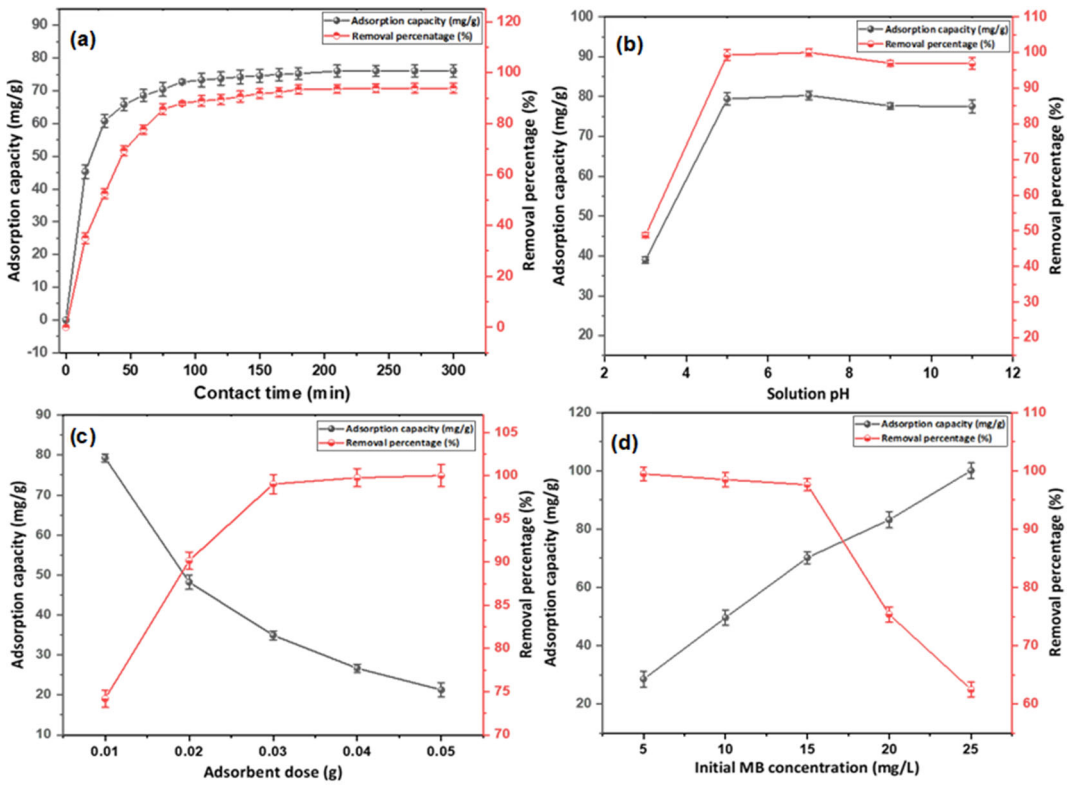

Fig 5. Effect of (a) contact time (b) solution pH (c) adsorbent dose and (d) initial concentration on adsorption of MB onto SRW

to evaluate the effect of contact time. As shown in Fig. 5(a), the adsorption capacity (Q_e) and removal percentage (%) are directly proportional to the adsorption time. As the adsorption time increased from 15 to 240 min, the adsorption capacity increased relatively rapidly from 45.33 to 76.08 mg/g, which could be due to the higher amount of active sites on SRW's surface that are vacant and available to interact with MB in the solution. However, within 300 min of the experiment, the vacant active sites on the surface of SRW was almost saturated or occupied, indicating that there is no increasing trend in adsorption capacity, and it becomes nearly constant. Therefore, the optimum adsorption equilibrium time of 300 min was chosen to be used throughout the adsorption experiments.

Effect of solution pH

The pH of a solution is an important parameter that affects the adsorption of adsorbate [2]. Fig. 5(b) illustrates the adsorption capacity and removal percentage of MB onto SRW (adsorbent) at various pH values under experimental conditions. The adsorption capacity of SRW increased from 39 mg/g to 80.3 mg/g when the pH was increased from 3 to 7. Then, the adsorption capacity slightly decreased from 77.65 mg/g to 77.55 mg/g as the pH rose from 9 to 11. Therefore, the adsorption mechanism could be electrostatic interaction between positively charged MB and negatively charged functional groups on the SRW surface. Thus. The adsorption process prefers basic/neutral media. We observed a low adsorption capacity in alkaline solution, which could be attributed to the large concentration of hydroxyl groups in the solution, which can compete with MB to attach to the adsorbent during the adsorption process. Ultimately, pH 7 was selected as the optimal solution pH for the adsorption studies.

Adsorbent dose effect

Fig. 5(c) depicts the trend of the MB adsorptive capacity with adsorbent dosage. As shown in Fig. 5(c), the adsorption capacity of SRW decreased from 79.3 mg/g to 21.29 mg/g as the adsorbent dose increased

from 0.01 to 0.05 g. An excess of adsorbent in the solution may promote agglomeration, decreasing the adsorption capacity since active adsorption sites are not completely occupied [14]. On the other hand, as the adsorbent dose was raised from 0.01 to 0.03 g, the removal percentage increased significantly from 74.18 to 99.03%, which could be attributed to the presence of more active sites on the adsorbent's surface that can capture the MB in the solution. Furthermore, as the dose of adsorbent material increased from 0.04 to 0.05 mg, the removal percentage of MB did not significantly increase, the removal percentage of MB did not significantly increase, which was due to the presence of fewer MB molecules in the solution. Finally, 30 mg of SRW was chosen to be the optimal adsorbent dosage for the adsorption experiments.

Effect of initial MB concentration

As illustrated in Fig. 5(d), the adsorption capacity increased from 28.5 mg/g to 100.05 mg/g as the initial MB concentration increased from 5 mg/L to 25 mg/L because high concentrations of MB in a solution leads to a greater adsorption driving force. On the other hand, As the concentration of MB increased, the removal efficiency of MB began to decline. This could be due to the number of accessible adsorption sites at a given dose of SRW was inadequate to adsorb a large number of MB molecules. Nonetheless, the higher removal percentage in diluted solutions could be attributed to the presence of enough active sites on the adsorbent's surface to accommodate a smaller number of MB molecules [19].

Kinetic Adsorption

To understand more about the adsorption process, the pseudo-first-order and pseudo-second-order reaction kinetic models were used to investigate the adsorption mechanisms of MB on SRW, as shown in Eq. (3) and (4).

$$\log(Q_e - Q_t) = \log Q_e - \frac{k_1}{2.303}t \quad (3)$$

$$\frac{t}{Q_t} = \frac{1}{Q_e}t + \frac{1}{k_2 Q_e^2} \quad (4)$$

where t (min) was the adsorption time, Q_e and Q_t (mg/g) were the adsorption capacity by SRW at equilibrium and time, respectively. And k_1 (1/min), and k_2 (g/(mg min)) were the pseudo-first-order and pseudo-second-order rate constants, respectively.

The kinetics of MB adsorption on SRW are depicted in Fig. 6(a) and (b). In addition, the experimental ($Q_{e,\,exp}$) and calculated ($Q_{e,\,cal}$) value of the adsorption capacity, adsorption kinetics parameters, and correlation coefficient are displayed in Table 3. As revealed, the correlation coefficient (R^2) for the pseudo-second-order model is higher than that pseudo-first-order one. The calculated adsorption capacity ($Q_{e,\,cal}$) obtained from pseudo-second-order is 78.78 mg/g which is close to the experimental adsorption capacity ($Q_{e,\,exp}$) of 77.21 mg/g. This indicates that the kinetics of MB adsorption by SRW is highly fitted with the pseudo-second-order of kinetics model.

Adsorption Isotherm

Adsorption isotherms describe the distribution of adsorbate molecules in the liquid phases at different equilibrium concentrations [10]. Finding an appropriate model that fits the adsorption data well yields important

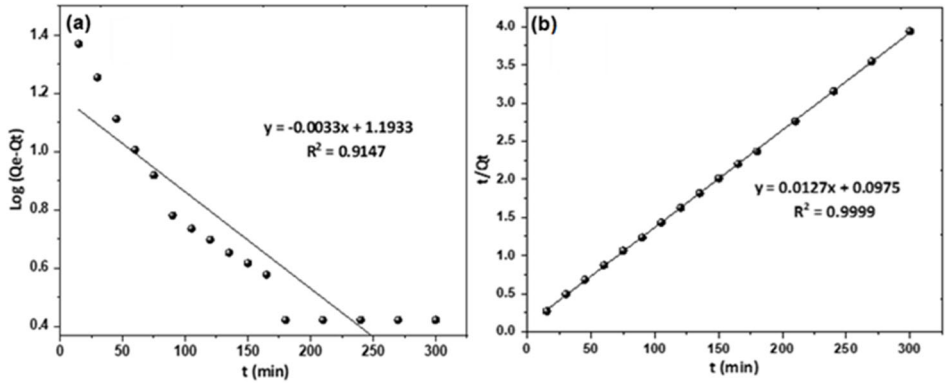

Fig 6. Adsorption kinetics; (a) Pseudo-first and (b) second-order kinetics

Table 3. Kinetic adsorption model parameters of adsorption MB onto SRW

$Q_{e,exp}$ (mg/g)	Pseudo-first order			Pseudo-second order		
	K_1 (min^1)	$Q_{e,cal}$ (mg/g)	R^2	K_2 (g/(mg min))	$Q_{e,cal}$ (mg/g)	R^2
77.21	0.0075	3.29	0.9147	0.0016	78.74	0.9999

insights into the adsorption process, such as how the interaction between adsorbent and adsorbate occurs. Langmuir [27] and Freundlich [10] are the most widely used adsorption models. These two models were used in their linear forms, as seen in Eq. (5) and (6):

$$\frac{C_e}{Q_e} = \frac{1}{Q_{max}K_L} + \frac{C_e}{Q_{max}} \quad (5)$$

$$\log Q_e = \log K_F + \frac{1}{n}\log C_e \quad (6)$$

where C_e (mg/L) is the equilibrium concentration of MB, Q_e (mg/g) is the amount of MB adsorbed per gram of adsorbent (SRW) under equilibrium, Q_{max} (mg/g) is the theoretical maximum adsorption capacity of SRW for MB, and K_L (L/mg) is a constant that describes the affinity in the Langmuir adsorption process; K_F (mg/g) is the Freundlich empirical constant that represents the SRW's relative adsorption capacity, and 1/n is a constant that represents the intensity of the Freundlich adsorption.

The adsorption equilibrium of MB onto SRW fits the Langmuir and Freundlich isotherms, as illustrated in Fig. 7(a) and (b), and the corresponding isotherm model constants and correlation coefficients (R^2) are reported in Table 4. The Langmuir isotherm model appropriately described the MB adsorption process on SRW due to the higher correlation coefficient (R^2 = 0.9994). Furthermore, the theoretical maximum adsorption capacity (Q_{max}) obtained from the Langmuir isotherm model was 119 mg/g, significantly greater than the experimental adsorption capacity. On the other hand, the correlation coefficient (R^2) of the Freundlich isotherm model was 0.9895, indicating that it was not suitable for portraying the adsorption process of MB onto SRW. The results revealed that MB adsorption onto SRW involves monolayer adsorption and that MB adsorption occurs on the energetically homogeneous surface of the SRW.

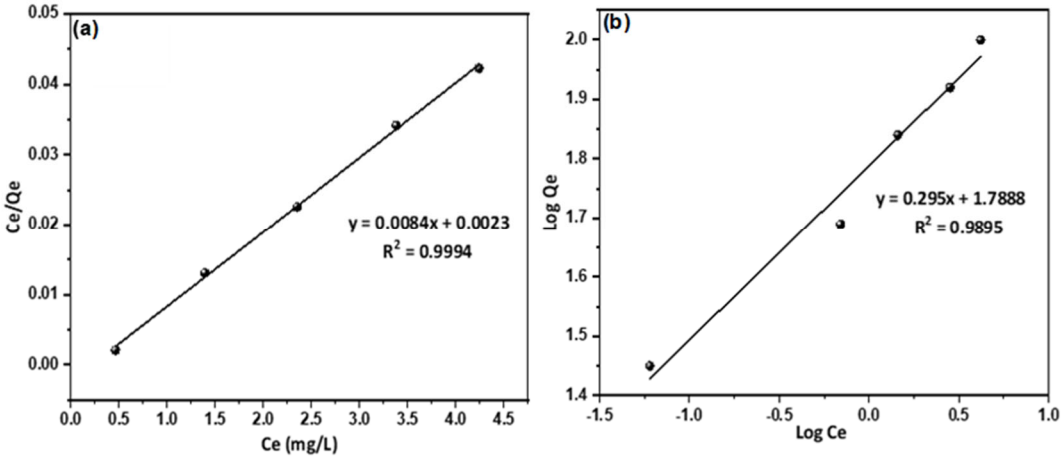

Fig 7. Adsorption isotherm; (a) Langmuir (b) Freundlich isotherms

Table 4. Langmuir and Freundlich isotherm parameter of MB adsorption onto SRW

Dye	Langmuir isotherm			Freundlich isotherm		
	Q_{max} (mg/g)	K_L (L/mg)	R^2	K_F (mg/g)	n	R^2
MB	119	3.65	0.9994	5.98	3.38	0.9895

The additional essential component in the Langmuir isotherm is a dimensionless constant known as the equilibrium parameter, which is as follows:

$$R_L = \frac{1}{1 + K_L C_o} \quad (7)$$

C_o denotes the initial MB concentration. The value of RL shows whether the isotherm model is reversible ($R_L = 0$), unfavorable ($R_L > 1$), linear ($R_L = 1$), or favorable ($0 < R_L < 1$). We calculated the R_L value and obtained $R_L = 0.1448$, suggesting that the adsorption is favorable.

Comparison of SRW with Other Adsorbent Materials

Waste-based adsorbents have previously been utilized to remove pollutants such as pharmaceuticals, dyes, and heavy metal ions. Similarly, polymeric adsorbent-derived rubber was used in this study to remove methylene blue from an aqueous solution. Table 5 shows the maximum adsorption capacity of SRW (119 mg/g), which is high compared to other adsorbent materials.

Regeneration and Reusability

The reusability and regeneration of adsorbents are essential factors in the decontamination process. We used adsorption steps in the reusability investigation with MB as the model pollutant. The adsorption processes are the same as those described in the experimental section. The adsorbent material was separated after adsorption by filtration with Whatman filter paper. The used adsorbent was taken for future reuse. For desorption, distilled water, 0.1 M HCl, and 0.1 M NaOH were used to desorb MB from SRW. The finding results demonstrated that SRW could be reused up to four times after the desorption process.

As seen in Fig. 8, SRW desorbed with 0.1 M NaOH had a higher removal percentage after four cycles (90.45 ± 2.07%) compared to 0.1 M HCl (42.32 ± 1.58%) and distilled water (12.34 ± 1.22%). The desorption efficiency at basic conditions indicates that an electrostatic interaction exists between the dye molecules and the aqueous solution. The high concentration of H^+ ions in 0.1 M HCl (pH 1~2) destructed the adsorbent structure, resulting in functional group collapse [29]. Therefore, 0.1 M NaOH (pH 11~12) increased the alkalinity of the aqueous solution, separating the adsorbed MB dye molecule that had been adsorbed on the adsorbent, resulting in a high percentage of dye removal.

■ CONCLUSION

This study showed that using sulfonated rubber waste (SRW) as a polymeric-adsorbent material is a good strategy for producing a promising low-cost adsorbent to

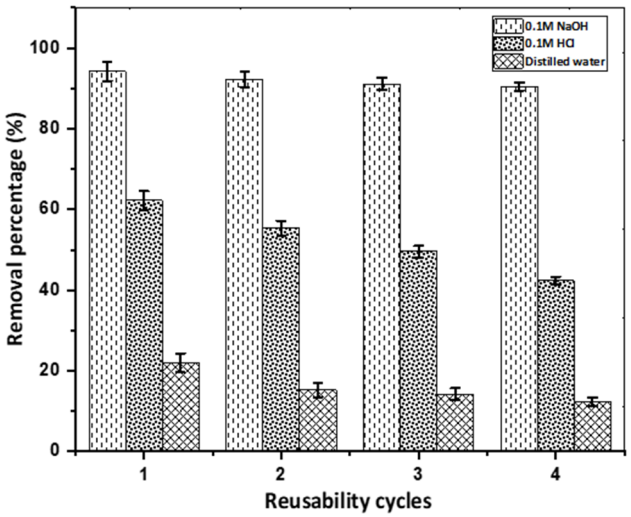

Fig 8. Reusability of SRW in 0.1 M NaOH, 0.1 M HCl, and distilled water

Table 5. Adsorption capacities toward methylene blue by some low-cost adsorbent materials

Adsorbent material	Adsorption capacity (mg/g)	References
R-NBR	60	[28]
Activated carbon	31.14	[2]
Cockle shells-treated banana pith	85.47	[17]
Spent rice biomass (SRB)	8.13	[9]
garlic peel	82.64	[24]
SRW	119	Present study

remove cationic MB dye from aqueous solutions, as well as a novel waste management method. After being modified with concentrated sulfuric acid, the sulfonate groups ($-SO_3^-$), was successfully added to the surface of SRW using a simple sulfonation method. The FESEM micrographs revealed that RW and SRW are spherical and irregular, with carbon, oxygen, and sulfur components dominating the elemental composition analysis (EDX). RW and SRW are both categorized as mesoporous materials based on their pore size distribution. The pH_{PZC} experiments revealed that RW and SRW have a neutral surface charge at pH 8.78 and 2.62, respectively. The experimental results revealed that SRW was highly dependent on operating parameters such as contact time, solution pH, adsorbent dose, and initial MB concentration. The parameters were optimized, and the data obtained were evaluated using various isotherm models (Langmuir and Freundlich) and kinetics models (pseudo-first and pseudo-second-order). Thus, the results of the adsorption experiments revealed that the Langmuir isotherm model was well fitted, with a maximum adsorption capacity of 119 mg/g and a better agreement with the pseudo-second-order kinetic model. Furthermore, SRW was proven to be highly reusable, with 0.1 M NaOH desorption being the optimal condition for reusability. Finally, SRW can be proposed as a cost-effective polymeric-adsorbent that can be used to treat dye-polluted wastewater.

■ ACKNOWLEDGMENTS

The authors would like to express their deepest gratitude to the management of Universiti Putra Malaysia and the Maikanya Foundation Hadejia for their generous support.

■ AUTHOR CONTRIBUTIONS

Muhammad Aliyu: Writing – review & editing. Abdul Halim Abdullah: Writing – review & editing. Mohamed Ibrahim Mohamed Tahir: Software. Muhammad Aliyu: Methodology, writing – original draft.

■ REFERENCES

[1] Nuzaimah, M., Sapuan, S.M., Nadlene, R., and Jawaid, M., 2018, Recycling of waste rubber as fillers: A review, *IOP Conf. Ser.: Mater. Sci. Eng.*, 368, 012016.

[2] Mahapatra, U., Chatterjee, A., Das, C., and Manna, A.K., 2021, Adsorptive removal of hexavalent chromium and methylene blue from simulated solution by activated carbon synthesized from natural rubber industry biosludge, *Environ. Technol. Innovation*, 22, 101427.

[3] Hirata, Y., Kondo, H., and Ozawa, Y., 2014, "Natural rubber (NR) for the tyre industry" in *Chemistry, Manufacture and Applications of Natural Rubber*, Woodhead Publishing, Cambridge, UK, 325–352.

[4] Bang-iam, N., Udnan, Y., and Masawat, P., 2013, Design and fabrication of artificial neural network-digital image-based colorimeter for protein assay in natural rubber latex and medical latex gloves, *Microchem. J.*, 106, 270–275.

[5] Mohammadi, M., Man, H.C., Hassan, M.A., and Yee, P.L., 2010, Treatment of wastewater from rubber industry in Malaysia, *Afr. J. Biotechnol.*, 9 (38), 6233–6243.

[6] Chakraborty, T.K., Islam, M.S., Zaman, S., Kabir, A.H.M.E., and Ghosh, G.C., 2020, Jute (*Corchorus olitorius*) stick charcoal as a low-cost adsorbent for the removal of methylene blue dye from aqueous solution, *SN Appl. Sci.*, 2 (4), 765.

[7] Temel, F., Turkyilmaz, M., and Kucukcongar, S., 2020, Removal of methylene blue from aqueous solutions by silica gel supported calix[4]arene cage: Investigation of adsorption properties, *Eur. Polym. J.*, 125, 109540.

[8] Jantawatchai, K., Jitpluem, S., Kerdlap, W., Phanawadee, P., Warakulwit, C., Chisti, Y., and Hansupalak, N., 2017, Production and characterization of a novel hierarchical porous silica adsorbent for removal of methylene blue dye from wastewaters, *Chem. Eng. Commun.*, 204 (12), 1452–1465.

[9] Saif ur Rehman, M., Kim, I., and Han, J.I., 2012, Adsorption of methylene blue dye from aqueous solution by sugar extracted spent rice biomass, *Carbohydr. Polym.*, 90 (3), 1314–1322.

[10] Olusegun, S.J., de Sousa Lima, L.F., and Mohallem, N.D.S., 2018, Enhancement of adsorption capacity of clay through spray drying and surface modification process for wastewater treatment, *Chem. Eng. J.*, 334.

[11] Kubra, K.T., Salman, M.S., and Hasan, M.N., 2021, Enhanced toxic dye removal from wastewater using biodegradable polymeric natural adsorbent, *J. Mol. Liq.*, 328, 115468.

[12] Huang, X.Y., Bu, H.T., Jiang, G.B., and Zeng, M.H., 2011, Cross-linked succinyl chitosan as an adsorbent for the removal of methylene blue from aqueous solution, *Int. J. Biol. Macromol.*, 49 (4), 643–651.

[13] Karagöz, S., Tay, T., Ucar, S., and Erdem, M., 2008, Activated carbons from waste biomass by sulfuric acid activation and their use on methylene blue adsorption, *Bioresour. Technol.*, 99 (14), 6214–6222.

[14] Islam, M.T., Saenz-Arana, R., Hernandez, C., Guinto, T., Ahsan, M.A., Bragg, D.T., Wang, H., Alvarado-Tenorio, B., and Noveron, J.C., 2018, Conversion of waste tire rubber into a high-capacity adsorbent for the removal of methylene blue, methyl orange, and tetracycline from water, *J. Environ. Chem. Eng.*, 6 (2), 3070–3082.

[15] Du, J.J., Yuan, Y.P., Sun, J.X., Peng, F.M., Jiang, X., Qiu, L.G., Xie, A.J., Shen, Y.H., and Zhu, J.F., 2011, New photocatalysts based on MIL-53 metal-organic frameworks for the decolorization of methylene blue dye, *J. Hazard. Mater.*, 190 (1-3), 945–951.

[16] Li, X., and Li, Y., 2019, Adsorptive removal of dyes from aqueous solution by $KMnO_4$-modified rice husk and rice straw, *J. Chem.*, 2019, 8359491.

[17] Hasan, R., Ying, W.J., Cheng, C.C., Jaafar, N.F., Jusoh, R., Jalil, A.A., and Setiabudi, H.D., 2020, Methylene blue adsorption onto cockle shells-treated banana pith: Optimization, isotherm, kinetic, and thermodynamic studies, *Indones. J. Chem.*, 20 (2), 368–378.

[18] Bello, O.S., Adegoke, K.A., Olaniyan, A.A., and Abdulazeez, H., 2015, Dye adsorption using biomass wastes and natural adsorbents: Overview and future prospects, *Desalin. Water Treat.*, 53 (5), 1292–1315.

[19] Hu, Z.P., Gao, Z.M., Liu, X., and Yuan, Z.Y., 2018, High-surface-area activated red mud for efficient removal of methylene blue from wastewater, *Adsorpt. Sci. Technol.*, 36 (1-2), 62–79.

[20] Chan, W.H., Mazlee, M.N., Ahmad, Z.A., Ishak, M.A.M., and Shamsul, J.B., 2017, The development of low-cost adsorbents from clay and waste materials: A review, *J. Mater. Cycles Waste Manage.*, 19 (1), 1–14.

[21] Troca-Torrado, C., Alexandre-Franco, M., Fernández-González, C., Alfaro-Domínguez, M., and Gómez-Serrano, V., 2011, Development of adsorbents from used tire rubber: Their use in the adsorption of organic and inorganic solutes in aqueous solution, *Fuel Process. Technol.*, 92 (2), 206–212.

[22] Nethaji, S., Sivasamy, A., and Mandal, A.B., 2013, Adsorption isotherms, kinetics and mechanism for the adsorption of cationic and anionic dyes onto carbonaceous particles prepared from Juglans regia shell biomass, *Int. J. Environ. Sci. Technol.*, 10 (2), 231–242.

[23] Ayodele, O.B., 2013, Effect of phosphoric acid treatment on kaolinite supported ferrioxalate catalyst for the degradation of amoxicillin in batch photo-Fenton process, *Appl. Clay Sci.*, 72, 74–83.

[24] Hameed, B.H., and Ahmad, A.A., 2009, Batch adsorption of methylene blue from aqueous solution by garlic peel, an agricultural waste biomass, *J. Hazard. Mater.*, 164 (2-3), 870–875.

[25] Foletto, V.S., Ferreira, A.B., da Cruz Severo, E., Collazzo, G.C., Foletto, E. L., and Dotto, G.L., 2017, Iron-based adsorbent prepared from Litchi peel biomass via pyrolysis process for the removal of pharmaceutical pollutant from synthetic aqueous solution, *Environ. Sci. Pollut. Res.*, 24 (11), 10547–10556.

[26] Jusoh, N.W.C., Choo, T.Y., Masudi, A., and Ali, R.R., 2020, Waste tire carbon adsorbent for active removal of paracetamol in aqueous solution, *J. Phys.: Conf. Ser.*, 1447, 012050.

[27] Dada, A.O., Olalekan, A.P., Olatunya, A.M., and Dada, O., 2012, Langmuir, Freundlich, Temkin and Dubinin–Radushkevich isotherms studies of equilibrium sorption of Zn^{2+} unto phosphoric acid

modified rice husk, *IOSR J. Appl. Chem.*, 3 (1), 38–45.

[28] Polat, K., and Bursalı, E.A., 2019, A promising strategy for the utilization of waste nitrile gloves: Cost-effective adsorbent synthesis, *J. Mater. Cycles Waste Manage.*, 21 (3), 659–665.

[29] Oladipo, A.C., Tella, A.C., Clayton, H.S., Olayemi, V.T., Akpor, O.B., Dembaremba, T.O., Ogunlaja, A.S., Clarkson, G.J., and Walton, R.I., 2021, A zinc-based coordination polymer as adsorbent for removal of trichlorophenol from aqueous solution: Synthesis, sorption and DFT studies, *J. Mol. Struct.*, 1247, 131274.